
Improving Graph Neural Network Expressivity via Subgraph Isomorphism Counting

Giorgos Bouritsas

Imperial College London
United Kingdom

g.bouritsas@imperial.ac.uk

Fabrizio Frasca

Twitter

United Kingdom

ffrasca@twitter.com

Stefanos Zafeiriou

Imperial College London
United Kingdom

s.zafeiriou@imperial.ac.uk

Michael M. Bronstein

Imperial College London / Twitter
United Kingdom

m.bronstein@imperial.ac.uk

Abstract

While Graph Neural Networks (GNNs) have achieved remarkable results in a variety of applications, recent studies exposed important shortcomings in their ability to capture the structure of the underlying graph. It has been shown that the expressive power of standard GNNs is bounded by the Weisfeiler-Lehman (WL) graph isomorphism test, from which they inherit proven limitations such as the inability to detect and count graph substructures. On the other hand, there is significant empirical evidence, e.g. in network science and bioinformatics, that substructures are often informative for downstream tasks, suggesting that it is desirable to design GNNs capable of leveraging this important source of information. To this end, we propose a novel topologically-aware message passing scheme based on subgraph isomorphism counting. We show that our architecture allows incorporating domain-specific inductive biases and that it is strictly more expressive than the WL test. Importantly, in contrast to recent works on the expressivity of GNNs, we do not attempt to adhere to the WL hierarchy; this allows us to retain multiple attractive properties of standard GNNs such as locality and linear complexity, while being able to disambiguate even hard instances of graph isomorphism. We extensively evaluate our method on graph classification and regression tasks and show state-of-the-art results on multiple datasets including molecular graphs and social networks.

1 Introduction

The field of graph representation learning has undergone a rapid growth in the past few years. In particular, Graph Neural Networks (GNNs), a family of neural architectures designed for irregularly structured data, have been successfully applied to problems ranging from social networks and recommender systems [1] to bioinformatics [2, 3], chemistry [4, 5, 6] and physics [7, 8], to name a few. Most GNN architectures are based on message passing [5], where at each layer the nodes update their hidden representations by aggregating information they collect from their neighbours.

A crucial difference from traditional neural networks operating on grid-structured data is the absence of canonical ordering of the nodes in a graph. To address this, usually the aggregation function is constructed to be invariant to neighbourhood permutations, and as a consequence, to graph isomorphism. This kind of symmetry is not always desirable, and thus different inductive biases that disambiguate the neighbours have been proposed. For instance, in geometric graphs, such as

3D molecular graphs and meshes, directional biases are usually employed in order to model the positional information of the nodes [9, 10, 11, 12, 13]; for proteins, ordering information is used to disambiguate amino-acids in different positions in the sequence [14]; in multi-relational knowledge graphs, a different aggregation is performed for each relation type [15].

The structure of the graph itself does not usually explicitly take part in the aggregation function. In fact, most models rely on multiple message passing steps as a means for each node to discover the global structure of the graph. However, this is not generally feasible, since it was proven that GNNs are at most as powerful as the Weisfeiler Lehman test (WL) [16, 17], that limiting their abilities to adequately exploit the graph structure, e.g. by counting substructures [18, 19]. This uncovers a crucial limitation of GNNs, as substructures have been widely recognised as important in the study of complex networks. For example, in molecular chemistry functional groups and rings are related to a plethora of chemical properties, while cliques are related to protein complexes in Protein-Protein Interaction networks and community structure in social networks, respectively.

In this work, we mark a first step in the direction of allowing graph neural models to learn topologically-aware representations of attributed graphs. We propose a structurally-biased message passing scheme, where each message is transformed differently depending on the topological relationship between the endpoint nodes. In order to achieve this, we construct structural identifiers that are assigned to either the vertices or the edges of the graph and are extracted by subgraph isomorphism counting. Intuitively, in this way we partition the nodes or the edges of each graph in different equivalence classes reflecting topological characteristics that are shared both between nodes in each graph individually and across different graphs. Our approach leverages domain-specific knowledge by choosing a collection of substructures that are known to be of importance in the graphs at hand (e.g. cliques for social networks or simple cycles for molecules). In this way, we model the most discriminative structural biases, which at the same time are amenable to generalisation. We show that our model is at least as powerful as traditional GNNs, while being strictly more expressive for the vast majority of substructures. Interestingly, certain substructures of small size can disambiguate strongly regular graphs, notable hard instances of graph isomorphism.

Contributions The main contributions of our paper are the following. First, we propose Graph Substructure Network (GSN), a novel structure-aware graph neural network architecture that encodes subgraph isomorphism counts. Second, we show that our approach increases GNN expressivity without having to follow the WL hierarchy (see section 2). Importantly, we retain the locality and linear computational complexity of traditional GNNs, as opposed to higher-order methods [20, 21, 22, 17]. Third, we show that in the limit, when the substructures are allowed to be almost the size of the graph, our model can yield a unique representation for every isomorphism class and is thus universal. Fourth, we provide an extensive experimental evaluation on both hard synthetic datasets (strongly regular graphs) as well as on real-world networks from the social and biological domains, including the recently introduced large-scale benchmarks [23, 24], where GSN achieves state-of-the-art results.

2 Preliminaries

Let $G = (\mathcal{V}_G, \mathcal{E}_G)$ be a graph with vertex set \mathcal{V}_G and undirected edge set \mathcal{E}_G . A subgraph $G_S = (\mathcal{V}_{G_S}, \mathcal{E}_{G_S})$ of G is any graph with $\mathcal{V}_{G_S} \subseteq \mathcal{V}_G$, $\mathcal{E}_{G_S} \subseteq \mathcal{E}_G$. When \mathcal{E}_{G_S} includes all the edges of G with endpoints in \mathcal{V}_{G_S} , i.e. $\mathcal{E}_{G_S} = \{(v, u) \in \mathcal{E} : v, u \in \mathcal{V}_{G_S}\}$, the subgraph is said to be *induced*.

Isomorphisms Two graphs G, H are *isomorphic* (denoted $H \simeq G$), if there exists an adjacency-preserving bijective mapping (*isomorphism*) $f : \mathcal{V}_G \rightarrow \mathcal{V}_H$, i.e. $(v, u) \in \mathcal{E}_G$ iff $(f(v), f(u)) \in \mathcal{E}_H$. Given some small graph H , the *subgraph isomorphism* problem amounts to finding a subgraph G_S of G such that $G_S \simeq H$. An *automorphism* of H is an isomorphism that maps H onto itself. The set of all the unique automorphisms form the *automorphism group* of the graph, denoted as $\text{Aut}(H)$ containing all the possible symmetries of the graph. The automorphism group yields a partition of the vertices into disjoint subsets of \mathcal{V}_H called *orbits*. Intuitively, this concept allows us to group the vertices based on their *structural roles*, e.g. the end vertices of a path, or all the vertices of a cycle (see Figure 1). Formally, the orbit of a vertex $v \in \mathcal{V}_H$ is the set of vertices to which it can be mapped via an automorphism: $\text{Orb}(v) = \{u \in \mathcal{V}_H : \exists g \in \text{Aut}(G) \text{ s.t. } g(u) = v\}$, and the set of

all orbits $H \setminus \text{Aut}(H) = \{\text{Orb}(v) : v \in \mathcal{V}_H\}$ is usually called the *quotient* of the automorphism when it acts on the graph H . We are interested in the unique elements of this set that we will denote as $\{O_{H,1}^V, O_{H,2}^V, \dots, O_{H,d_H}^V\}$, where d_H is the cardinality of the quotient.

Analogously, we define edge structural roles via *edge automorphisms*, i.e. bijective mappings from the edge set onto itself, that preserve edge adjacency (two edges are adjacent if they share a common endpoint). In particular, every vertex automorphism g induces an edge automorphism by mapping each edge $\{u, v\}$ to $\{g(u), g(v)\}$.¹ In the same way as before, we construct the edge automorphism group, from which we deduce the partition of the edge set in *edge orbits* $\{O_{H,1}^E, O_{H,2}^E, \dots, O_{H,d_H}^E\}$.

Weisfeiler-Lehman tests The *Weisfeiler-Lehman graph-isomorphism test* [26], or naive vertex refinement (we will refer to it as *1-WL* or just *WL*), is a fast heuristic to decide if two graphs are isomorphic. The WL test proceeds as follows: every vertex v is initially assigned a colour $c^0(v)$ that is later iteratively refined by aggregating neighbouring information:

$$c^{t+1}(v) = \text{HASH}\left(c^t(v), \mathcal{Z}(c^t(u))_{u \in \mathcal{N}(v)}\right), \quad (1)$$

where $\mathcal{Z}(\cdot)$ denotes a multiset (a set that allows element repetitions) and $\mathcal{N}(v)$ is the neighbourhood of v . Note that the neighbour aggregation in the WL test is a form of message passing, and GNNs are the learnable analogue.

Most of the research in improving GNN expressivity has focused on models that mimic the generalisations of WL, known as the WL hierarchy. Briefly, here we describe the so-called *Folklore WL family* (*k-FWL*), as referred to by Maron et al. [22].² The *k-FWL* operates on *k*-tuples of nodes $\mathbf{v} = (v_1, v_2, \dots, v_k)$ to which an initial colour $c^0(\mathbf{v})$ is assigned based on their *isomorphism types*, which can loosely be thought of as a generalisation of isomorphism that also preserves the ordering of the nodes in the tuple (see supplementary material). Then, at each iteration the colour is refined as follows:

$$c^{t+1}(\mathbf{v}) = \text{HASH}\left(c^t(\mathbf{v}), \mathcal{Z}(c^t(\mathbf{v}_{u,1}), c^t(\mathbf{v}_{u,2}), \dots, c^t(\mathbf{v}_{u,k}))_{u \in \mathcal{V}}\right), \quad (2)$$

where $\mathbf{v}_{u,j} = (v_1, v_2, \dots, v_{j-1}, u, v_{j+1}, \dots, v_k)$.

The multiset $\mathcal{Z}(c^t(\mathbf{v}_{u,1}), c^t(\mathbf{v}_{u,2}), \dots, c^t(\mathbf{v}_{u,k}))_{u \in \mathcal{V}}$ can be perceived as a form of generalised neighbourhood. Note here, that information is saved in all possible tuples in the graph, thus each *k*-tuple receives information *from the entire graph*, contrary to the *local* nature of the 1-WL test. Regarding the order *k* of each test in the hierarchy, it is known that $(k+1)$ -FWL is strictly stronger than *k*-FWL and that 2-FWL is strictly stronger than the simple 1-WL test.

3 Graph Substructure Networks

Complex networks consist of nodes (or edges) with repeated structural roles. Thus, it is natural for a neural network to treat them in a similar manner, akin to weight sharing between local patches in CNNs for images [29] or positional encodings in language models for sequential data [30, 31, 32].

However, contrary to Euclidean domains (regular 2D and 1D grids underlying image or text data), the diversity in the topology of such networks prohibits modelling each structural role independently, as that would be inefficient and a large amount of training data would be required. In other words, if one attempted to model the structural role of node v by examining the isomorphism class of a neighbourhood $\mathcal{N}(v)$ of certain radius around v , there will typically be an insufficient number of training examples per class. To address this, we suggest a simplification where nodes are described by *vertex invariants*, features that are invariant to isomorphism but also possibly shared between different isomorphism classes.

Such invariants are naturally extracted by GNNs themselves, but it can be argued that they might be oversimplified, as nodes will be blind to the existence of e.g. triangles or larger cycles in

¹Note that the edge automorphism group is larger than that of induced automorphisms, but strictly larger only for 3 trivial cases [25]. However, induced automorphisms provide a more natural way to express structural roles.

²In the majority of papers on GNN expressivity [17, 22, 19], another family of WL tests is discussed, under the terminology *k-WL* with expressive power equal to $(k-1)$ -FWL. In contrast, in most graph theory papers on graph isomorphism [27, 28, 18] the *k-WL* term is used to describe the algorithms referred to as *k-FWL* in GNN papers. Here, we follow the *k-FWL* convention to align with the work mostly related to ours.

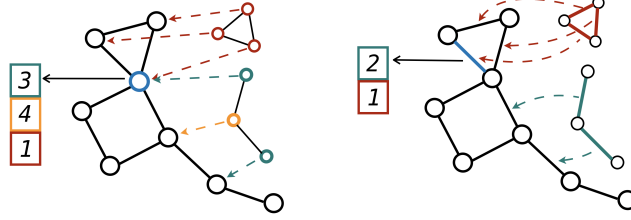


Figure 1: *Node* (left) and *edge* (right) induced subgraph counting for a 3-cycle and a 3-path. Counts are reported for the blue node on the left and for the blue edge on the right. Different colors depict orbits.

their neighbourhoods [19, 18]. Hence, we propose to extend GNNs towards inferring a stronger invariant that will be able to capture richer topological properties. In particular, we observe that the neighbourhood of each node can be partially described by its substructures, thus by counting their appearances, one obtains an approximate characterisation of the node’s structural role. This information can be subsequently passed to a GNN and act in a complementary manner.

Structural features Let $\mathcal{H} = \{H_1, H_2 \dots H_K\}$ be a set of small (connected) graphs, for example cycles of fixed length or cliques. For each graph $H \in \mathcal{H}$, we first find its isomorphic subgraphs in G ; let f be a subgraph isomorphism between H and G_S . For each node $v \in \mathcal{V}_{G_S}$ we infer its role w.r.t. H by obtaining the orbit of its mapping $f(v)$ in H , $\text{Orb}_H(f(v))$. By counting all the possible appearances of different orbits in v , we obtain the *structural feature* $\mathbf{x}_H^V(v)$ of v , defined as follows:

$$x_{H,i}^V(v) = \frac{|\{G_S \simeq H : v \in \mathcal{V}_{G_S} \text{ s.t. } f(v) \in O_{H,i}^V\}|}{|\text{Aut}(H)|}, \quad i = 1, \dots, d_H. \quad (3)$$

We divide the counts by the number of the automorphisms of H , since for every matched subgraph G_S there will always be $|\text{Aut}(H)|$ different ways to map it to H , thus these repetitions will be uninformative. By combining the counts from different substructures in \mathcal{H} and different orbits, we obtain the feature vector $\mathbf{x}_V(v) = [\mathbf{x}_{H_1}^V(v), \dots, \mathbf{x}_{H_K}^V(v)] \in \mathbb{N}^{D \times 1}$ of dimension $D = \sum_{H_i \in \mathcal{H}} d_{H_i}$.

Similarly, we can define *edge structural features* $\mathbf{x}_{H,i}^E(\{u, v\})$ by counting occurrences of edge automorphism orbits:

$$x_{H,i}^E(\{u, v\}) = \frac{|\{G_S \simeq H : \{u, v\} \in \mathcal{E}_{G_S} \text{ s.t. } \{f(u), f(v)\} \in O_{H,i}^E\}|}{|\text{Aut}(H)|}, \quad (4)$$

and the combined edge features $\mathbf{x}_E(\{u, v\}) = [\mathbf{x}_{H_1}^E(\{u, v\}), \dots, \mathbf{x}_{H_K}^E(\{u, v\})]$. An example of vertex and edge structural features is illustrated in Figure 1.

Structure-aware message passing The key building block of our architecture is the graph sub-structure layer, defined in a general manner as a Message Passing Neural Network (MPNN) [5], where now the messages from the neighbouring nodes also contain the structural information. In particular, each node v updates its state $\mathbf{h}^t(v)$ by combining its previous state with the aggregated messages: $\mathbf{h}^{t+1}(v) = \text{UP}^{t+1}(\mathbf{h}^t(v), \text{MSG}^{t+1}(v))$, where the UP^{t+1} function is a neural network (multilayer perceptron - MLP) and the message aggregation is a summation of features transformed by an MLP M^{t+1} as follows:

$$\text{MSG}^{t+1}(v) = \sum_{u \in \mathcal{N}(v)} M^{t+1}(\mathbf{h}^t(v), \mathbf{h}^t(u), \mathbf{x}_V(v), \mathbf{x}_V(u), \mathbf{e}(\{u, v\})) \quad (5)$$

$$\text{MSG}^{t+1}(v) = \sum_{u \in \mathcal{N}(v)} M^{t+1}(\mathbf{h}^t(v), \mathbf{h}^t(u), \mathbf{x}_E(\{u, v\}), \mathbf{e}(\{u, v\})) \quad (6)$$

where the two variants, named *GSN-v* and *GSN-e*, correspond to vertex- or edge-counts, respectively, and $\mathbf{e}(\{u, v\})$ denotes edge features.

How powerful are GSNs? We now turn to the expressive power of GSNs in comparison to the classical WL graph isomorphism tests, a key tool for the theoretical analysis of the expressivity of graph neural networks so far.

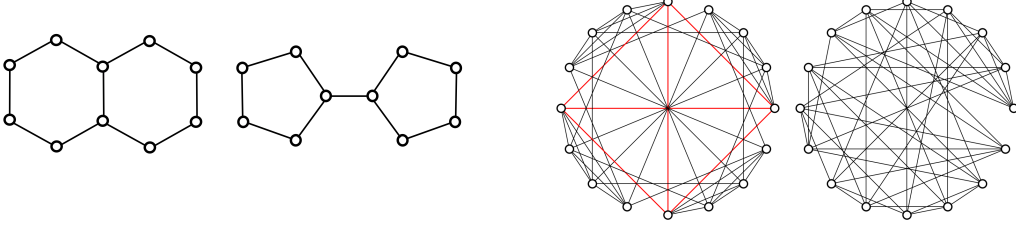


Figure 2: (Left) *Decalin* and *Bicyclopentyl*: Non-isomorphic molecular graphs than can be distinguished by GSN, but not the by the WL test [33] (nodes represent carbon atoms and edges chemical bonds). (Right) *Rook's 4x4 graph* and the *Shrikhande graph*: the smallest pair of SR non-isomorphic graphs with the same parameters $SR(16,6,2,2)$. GSN can distinguish them with 4-clique counts, while 2-FWL fails.

Proposition 3.1. *GSNs are at least as powerful as MPNNs and the 1-WL test.*

Proof. The first part of the proof is trivial since the GSN model class contains MPNNs and is thus at least as expressive. For the 1-WL test, one can repurpose the proof of Theorem 3 in [16] and demand the injectivity of the update function (w.r.t. both the hidden state $\mathbf{h}^t(v)$ and the message aggregation $\text{MSG}^{t+1}(v)$), and the injectivity of the message aggregation w.r.t. the multiset of the hidden states of the neighbours $\{\mathbf{h}^t(u)\}_{u \in \mathcal{N}(v)}$. It suffices then to show that if injectivity is preserved then GSNs are at least as powerful as the 1-WL. \square

Furthermore, we can state that GSNs have the capacity to learn functions that traditional MPNNs cannot learn. The following observation derives directly from the analysis of the counting abilities of the 1-WL test [18] and its extension to MPNNs [19].

Proposition 3.2. *GSNs are strictly more powerful than MPNNs and the 1-WL test when H is any induced subgraph except from single edges and single nodes, or any not necessarily induced subgraph except from star graphs of any size.*

Proof. Arvind et al. [18] showed that 1-WL, and consequently MPNNs, can count only *forests of stars*. Thus, if the subgraphs are required to be connected, then they can only be star graphs of any size (note that this contains single nodes and single edges). In addition, Chen et al. [19], showed that 1-WL, and consequently MPNNs, cannot count any connected induced subgraph with 3 or more nodes, i.e. any connected subgraph apart from single nodes and single edges.

Given proposition 3.1, in order to show that GSNs are strictly more expressive than MPNNs and the 1-WL test, it suffices to show that GSN can distinguish a pair of graphs that MPNNs and the 1-WL test deem isomorphic. If H is a substructure that MPNNs cannot learn to count, i.e. the ones mentioned above, then there is at least one pair of graphs with different number of counts of H , that MPNNs deem isomorphic. Thus, by assigning counting features to the nodes/edges of the two graphs based on appearances of H , a GSN can obtain different representations for G_1 and G_2 by summing up the features. Hence, G_1, G_2 are deemed non-isomorphic. An example is depicted in Figure 2 (left), where the two non-isomorphic graphs are distinguishable by GSN via e.g. cycle counting, but not by 1-WL. \square

Although our method does not attempt to align with the WL hierarchy, we observe that it has the capacity to distinguish graphs where the 2-FWL fails, which can be stated as:

Proposition 3.3. *2-FWL is not stronger than GSN.*

Proof. It is sufficient to find an example of two non-isomorphic graphs that are distinguishable by GSN but not by 2-FWL, for which purpose let us consider the following family of graphs:

Definition 3.1 (Strongly regular graph). *A $SR(n,d,\lambda,\mu)$ -graph is a regular graph with n nodes and degree d , where every two adjacent vertices have always λ mutual neighbours, while every two non-adjacent vertices have always μ mutual neighbours.*

The graphs in Figure 2 (right) are examples of non-isomorphic strongly regular graphs, on which 2-FWL (and thus 1-WL) tests are known to fail. 2-FWL will always decide that a pair of SR graphs with the same parameters n, d, λ, μ are isomorphic, since all 2-tuples of the same isomorphism type have the exact same generalised neighbourhood, leading 2-FWL to converge to its solution at initialisation (a detailed proof is provided in the supplementary material). On the other hand, the examples of Figure 2 can be distinguished by a GSN by e.g. counting 4-cliques: there is at least one in Rook’s 4x4 graph contrary to the Shrikhande graph that has none. \square

In fact, in Section 5.1, we empirically show that small-sized substructures are usually adequate to tell strongly regular graphs apart. Although it is not clear if there exists a certain substructure collection that results in GSNs that align with the WL hierarchy, we stress that this is not a necessary condition in order to design more powerful GNNs. In particular, the advantages offered by k -WL might not be able to outweigh the disadvantage of the larger computational complexity introduced. For example, a 2-FWL equivalent GNN will still fail to count 4-cliques (a frequent pattern in social and biological networks) or 8 cycles (a common ring structure in organic molecules). Therefore, we suggest that it might be more appropriate to design powerful GNNs based on the distinct characteristics of the task at hand.

How large should the substructures be? An interesting question that arises is which substructures are most *informative* and whether they can completely characterise the graph. As of today, we are not aware of any results in graph theory that can guarantee the reconstruction of a graph from a smaller collection of its subgraphs. In fact, the Reconstruction Conjecture [34, 35], states that a graph with size $n \geq 3$ can be reconstructed from its vertex-deleted subgraphs, which in our case amounts to using all the substructures of size $k = n - 1$. Therefore, if the Reconstruction Conjecture holds, GSN can distinguish all non-isomorphic graphs when using substructures of size $k = n - 1$. However, the Reconstruction Conjecture has only been proven for $n \leq 11$ [36] and still remains open for larger graphs, while to the best of our knowledge, there is no similar hypothesis for smaller values of k . Furthermore, we hypothesise that for ML tasks, too large subgraphs might lead to overfitting, while in practice small structures of size $k = \mathcal{O}(1)$ are sufficient. This is validated by the experiments where strong empirical performance is observed for small and relatively frequent subgraph structures.

Complexity In the general case, subgraph isomorphism is a NP-complete problem, while its counting version is $\#P$ -Complete [37]. However, for fixed k values, the setting we are interested in, the problem can be solved in $\mathcal{O}(n^k)$ by examining all the possible k -tuples in the graph. For specific types of subgraphs, such as paths and cycles, the problem can be solved even faster (see e.g. [38]). Moreover, the computationally expensive part of the algorithm is done as a preprocessing step and thus does not affect network training and inference that remain linear w.r.t the number of edges, $\mathcal{O}(|\mathcal{E}|)$. This is opposed to k -WL equivalents [22, 17] with $\mathcal{O}(n^k)$ training complexity and relational pooling [39] with $\mathcal{O}(n!)$ training complexity in absence of approximations.

4 Related Work

Expressive power of GNNs and the WL hierarchy The seminal results in the theoretical analysis of the expressivity of GNNs [16] and k -GNNs [17] established that traditional message passing-based GNNs are at most as powerful as the 1-WL test. Chen et al. [40] showed that graph isomorphism is equivalent to universal invariant function approximation. Maron et al. [20, 21, 22] studied Invariant Graph Networks (IGN) - compositions of Invariant linear layers interleaved with non-linear activation functions - constructed to be invariant to symmetry groups. Subsequently it was argued [21, 41] that in order for this construction to be universal, it must involve tensors of order no less than linear w.r.t. the graph size n . Given the obvious impractical consequences of this result, IGNs were studied in the context of the WL hierarchy [22], similarly to [17]; it was shown that k -order IGNs are as expressive as k -WL. In addition, the authors proposed a 2-FWL equivalent variant, based on matrix multiplication, instead of linear invariant layers. A similar construction is Ring-GNN, proposed in [40]. The main drawback of these methods is the complexity and memory requirements of $\mathcal{O}(n^k)$, and the number of parameters for linear IGNs of $\mathcal{O}(B_k)$ (bell number), making them impractical.

From a different perspective, Sato et al. [42] and Loukas [43] showed the connections between GNNs and distributed local algorithms [44, 45, 46] and suggested more powerful alternatives employing either port numberings, i.e. local orderings, that make GNNs more powerful than the 1-WL test,

or unique global identifiers, that make GNNs universal. It was later shown that using random features [47] can serve this role and allow node disambiguation in GNNs. However, these methods lack a principled way to choose orderings/identifiers so as to be shared across graphs (this would require a graph canonisation procedure). Other proposed methods [39] take into account all possible node permutations and can therefore be intractable; required approximations are at the cost of compromising expressivity.

Solely quantifying the expressive power of GNNs in terms of their ability to distinguish non-isomorphic graphs does not provide the necessary granularity: even the 1-WL test can distinguish almost all (in the probabilistic sense) non-isomorphic graphs [48]. Chen et al. [19] approached GNN expressivity by studying their ability to *count substructures*. Similarly, for the k -WL tests, there have been efforts to analyse their power as graph invariants [49, 28, 18, 50]. It was established, for example, that the 2-FWL test is more powerful than spectral invariants [49], can count cycles and paths of length up to 7, but not 4-cliques [28, 18], while the k -FWL test can count the number of subgraph homomorphisms of treewidth up to k [50]. These characterisations of expressivity are more intuitive and informative and serve as our motivation for the design of more powerful architectures. We refer the interested reader to a recent survey on GNN expressivity for an extensive discussion [33].

Substructures in Complex Networks The idea of analysing complex networks based on small-scale topological characteristics dates back to the 1970’s and the notion of triad census for directed graphs [51]. The seminal paper of Milo et al. [52] coined the term *network motifs* as over-represented subgraph patterns that were shown to characterise certain functional properties of complex networks in systems biology. This idea has since been successfully applied to study the higher organisation of transportation and neuronal networks [53], temporal networks [54], and molecules [55, 56, 57]. The closely related concept of *graphlets* [58, 59, 60, 61], different from motifs in being induced subgraphs, has been used to analyse the distribution of real-world networks and as a topological signature for network similarity. Our work is similar in spirit with the *graphlet degree vector* (GDV) [59], a node-wise descriptor based on graphlet counting. In our work, we endeavour to combine these ideas with message passing, so as to learn richer representations by diffusing structural descriptors along with node and edge attributes through the graph.

Substructures have been also used in the context of ML. In particular, subgraph patterns have been used to define Graph Kernels (GKs) [62, 63, 64, 65], with the most prominent being the graphlet kernel [63], based on counting the occurrences of all possible induced subgraphs of a maximum fixed size. In comparison to GNNs, these methods usually only extract graph-level representations and not node-level. Motif-based node embeddings [66, 67] and diffusion operators [68, 69, 70] that employ adjacency matrices weighted according to motif occurrences, have recently been proposed for graph representation learning; these can be expressed by our general formulation. Finally, GNNs that operate in larger induced neighbourhoods [71, 72] or higher-order paths [73] have prohibitive complexity since the size of these neighbourhoods typically grows exponentially.

5 Experimental Evaluation

In the following section we evaluate GSN in comparison to the state-of-the-art in a variety of datasets from different domains. We are interested in empirically assessing if the generalisation capabilities of our method in real-world scenarios are in agreement with its expressive power. Most importantly, we are interested in practical scenarios where the collection of subgraphs, as well as their size, are kept small. This section is structured as follows: a) Synthetic experiment, where we show the capabilities of our method in distinguishing hard instances of non-isomorphic graphs, b) graph classification experiments in the TUD benchmark datasets (social and biological networks), c) evaluation on novel graph benchmarks: graph regression on the ZINC molecular dataset by [23] and graph classification on the ogbg-molhiv molecular dataset from the recently introduced Open Graph Benchmark [24].

Depending on the dataset domain we experimented with different substructure families (*cycles*, *paths* and *cliques*) and maximum substructure size k (note that for each setting, our substructure collection consists of all the substructures of the family with size $\leq k$). We also experimented with both graphlets and motifs and observed similar performance in most cases. Please refer to the supplementary material for additional details on the experimental setup.

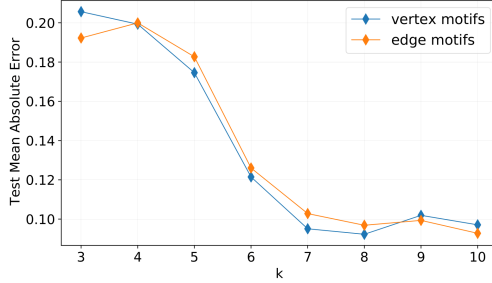


Figure 3: GSN performance with k -cycle motifs on ZINC.

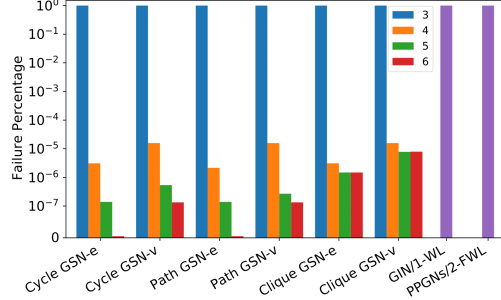


Figure 4: SR graphs isomorphism test (log scale). Different colours indicate different substructure sizes.

5.1 Synthetic Experiment - Graph Isomorphism test

In the following experiment we tested the ability of GSNs to decide if two graphs are non-isomorphic. We use a collection of Strongly Regular graphs³ of size up to 35 nodes and attempt to disambiguate pairs with the same number of nodes (for different sizes the problem becomes trivial). At this stage we are only interested in the bias of the architecture itself, we thus use GSN with random weights to compute graph representations. Two graphs are deemed isomorphic if the euclidean distance of their representations is smaller than a predefined threshold ϵ . Figure 4 shows the failure percentage of our isomorphism test when using different graphlet substructures (*cycles*, *paths*, and *cliques*) of varying size k . Interestingly, the number of failure cases of GSN decreases rapidly as we increase k ; cycles and paths of maximum length equal to 6 are enough to tell apart all the graphs in the dataset. Note that the performance of cliques saturates, possibly because the largest clique in our dataset has 5 nodes. Observe also the discrepancy between GSN-v and GSN-e. In particular, vertex-wise counts do not manage to distinguish all graphs, although missing only a few instances. We hypothesise that this is because edge counts offer a higher level of granularity, allowing GSN to create a finer partition of the nodes in the graph. Finally, 1-WL and 2-FWL equivalent models demonstrate 100% failure, as expected from theory.

5.2 TUD Graph Classification Benchmarks

In the following section, we evaluate our method on datasets from the classical TUD benchmarks.⁴ This is a large collection of datasets from various domains, that have been widely used in the evaluation of graph-related ML approaches.

We use seven datasets from the domains of bioinformatics and computational social science and compare against various GNNs and Graph Kernels. Our main GNN baselines are GIN [16] and PPGNs [22]. We follow the same evaluation protocol of [16], i.e. we perform 10-fold cross-validation and then report the performance at the epoch with the best average accuracy across the 10 folds. Table 1 lists all the methods evaluated with the split of [74]. We select our model by tuning architecture and optimisation hyperparameters and substructure related parameters: 1) k , 2) motifs against graphlets. Following domain evidence we choose the following substructure families: *cycles* for molecules, *cliques* for social networks. Best performing substructures both for GSN-e and GSN-v are reported. As can be seen, our model obtains state-of-the-art performance in most of the datasets, while in some cases by a considerable margin when compared to the main GNN baselines. The only case where PPGNs outperform GSNs is the *Proteins* dataset, which we conjecture is due to a lack of prominent structural patterns. Note that in *Proteins*, every datapoint is a graph-based model of the 3D conformation of a protein (nodes are secondary structures), thus graph substructures are not expected to strongly correlate with the task.

³Available from <http://users.cecs.anu.edu.au/~bdm/data/graphs.html>

⁴Available from <https://chrsmrrs.github.io/datasets/>

Table 1: Graph classification accuracy on various social and biological networks from the TUD Dataset collection. The top three performance scores are highlighted as: **First**, **Second**, **Third**. For GSN, we show the best performing substructure collection. * denotes Graph Kernel methods.

Dataset	MUTAG	PTC	Proteins	NC11	Collab	IMDB-B	IMDB-M
RWK* [75]	79.2±2.1	55.9±0.3	59.6±0.1	>3 days	N/A	N/A	N/A
GK* (k=3) [63]	81.4±1.7	55.7±0.5	71.4±0.31	62.5±0.3	N/A	N/A	N/A
PK* [76]	76.0±2.7	59.5±2.4	73.7±0.7	82.5±0.5	N/A	N/A	N/A
WL kernel* [77]	90.4±5.7	59.9±4.3	75.0±3.1	86.0±1.8	78.9±1.9	73.8±3.9	50.9±3.8
GNTK* [78]	90.0±8.5	67.9±6.9	75.6±4.2	84.2±1.5	83.6±1.0	76.9±3.6	52.8±4.6
DCNN [79]	N/A	N/A	61.3±1.6	56.6±1.0	52.1±0.7	49.1±1.4	33.5±1.4
DGCNN [74]	85.8±1.8	58.6±2.5	75.5±0.9	74.4±0.5	73.8±0.5	70.0±0.9	47.8±0.9
IGN [20]	83.9±13.	58.5±6.9	76.6±5.5	74.3±2.7	78.3±2.5	72.0±5.5	48.7±3.4
GIN [16]	89.4±5.6	64.6±7.0	76.2±2.8	82.7±1.7	80.2±1.9	75.1±5.1	52.3±2.8
PPGNs [22]	90.6±8.7	66.2±6.6	77.2±4.7	83.2±1.1	81.4±1.4	73.0±5.8	50.5±3.6
GSN-e	90.6±7.5	68.2±7.2	76.6±5.0	83.5±2.3	85.5±1.2	77.8±3.3	54.3±3.3
6 (cycles)	6 (cycles)	6 (cycles)	4 (cliques)	15 (cycles)	3 (triangles)	5 (cliques)	5 (cliques)
GSN-v	92.2±7.5	67.4±5.7	74.6±5.0	83.5±2.0	82.7±1.5	76.8±2.0	52.6±3.6
12 (cycles)	10 (cycles)	4 (cliques)	3 (triangles)	3 (triangles)	4 (cliques)	3 (triangles)	

5.3 Evaluation on novel Graph Benchmarks

Recently, there has been criticism on the reliability of the TUD datasets, mainly due to their small size, isomorphism bias and the evaluation procedure [80, 81]. In accordance with that, we also evaluated our method on datasets from two recently introduced benchmarks: *ZINC* from the benchmark introduced in [23] and *ogbg-molhiv* from the Open Graph Benchmark (OGB) [24]. Both are new initiatives attempting to tackle the aforementioned problems with a diverse collection of medium and large scale graph datasets associated with a variety of tasks and a standardised evaluation protocol.⁵

ZINC We evaluate on molecules from the ZINC database [82, 83, 84, 85, 23], where the task is to regress their constrained solubility property. Our main baselines are GIN (which we re-implement), as well as a stronger baseline (as in Eq. 5 and 6 without structural features - see supplementary material for details) that can also take into account edge features (MPNN^E). Then we extend both baselines with structural features obtained with *k*-cycle counting (models denoted as GSN and GSN^E) and report the result of the best performing substructure w.r.t. the validation set. The data split into training, validation and test set is obtained from [23]. We also follow the same evaluation protocol of [23], i.e. we reduce the learning rate when the validation loss is not improving and stop the training when the learning rate reaches a minimum predefined value - validation and test metrics are inferred using the model at the last training epoch. The evaluation metric (as well as training loss) is Mean Absolute Error (MAE). Table 2 shows that our model significantly outperforms all the baselines. In Figure 3 we show the test performance of GSN when changing the maximum cyclical substructure size, and observe that the model starts improving substantially when $k \geq 6$. This is expected, as cyclical patterns of such sizes (e.g. aromatic rings) are very common in organic molecules.

OGB-MOLHIV We focus on a graph-level prediction dataset, the *ogbg-molhiv*, where the aim is to predict if a molecule inhibits HIV replication or not (binary classification). Note that this dataset comprises a challenge for ML models, due to the fact that the data are split based on the 2D structure of the molecules (this process is known in chemistry as scaffolding), that is molecules with different structure belong to different subsets. With this choice, the authors simulate a more realistic setting that allows to test a model’s capacity in extrapolating beyond the given data distribution. The baseline architecture provided by the authors is a variation of GIN that allows for edge features and is extended with a *virtual node*, *GIN-VN*, or with additional node/edge features, *GIN-AF*, or both, *GIN-VN-AF* (more information in the supplementary material). Similarly with the experiment on ZINC, we extend the baseline settings with cyclical substructure features by treating them in a similar way as node and edge features (*GSN-VN*, *GSN-AF*, *GSN-VN-AF*). Using the evaluator provided by the authors, we report the ROC-AUC metric at the epoch with the best validation performance (substructures are also chosen based on the validation set). As can be seen from Table 3, considerable improvement in the performance of the model in all splits is obtained, thus demonstrating strong generalisation

⁵further information at <https://github.com/graphdeeplearning/benchmarking-gnns> and <https://ogb.stanford.edu/> respectively

Table 2: MAE on *ZINC*. ‘*E*’: edge features. †Our GIN implementation.

Method	Test MAE
GCN [86]	0.469±0.002
GAT [87]	0.463±0.002
GIN [16]	0.408±0.008
GatedGCN ^E [88]	0.363±0.009
GIN [†]	0.288±0.011
MPNN ^E	0.184±0.012
GSN	0.139±0.007
GSN^E	0.108±0.018

Table 3: ROC-AUC on ogbg-molhiv. ‘-AF’: Additional features, ‘-VN’: message passing with a virtual node.

Method	Training	Validation	Test
GCN-VN	88.65±1.01	83.73±0.78	74.18±1.22
GCN-AF	88.65±2.19	82.04±1.41	76.06±0.97
GCN-VN-AF	90.07±4.69	83.84±0.91	75.99±1.19
GIN-VN	93.89±2.96	84.1±1.05	75.2±1.30
GIN-AF	88.64±2.54	82.32±0.90	75.58±1.40
GIN-VN-AF	92.73±3.80	84.79±0.68	77.07±1.49
GSN-VN	93.61±1.85	84.45±0.97	75.88±1.86
GSN-AF	88.67±3.26	85.17±0.90	76.06±1.74
GSN-VN-AF	94.30±3.38	86.58±0.84	77.99±1.00

capabilities. Tests with additional chemical features such as formal charge, hybridisation, etc. (‘-AF’ setting in Table 3) show that structure provides important complementary information.

6 Conclusion

In this paper, we propose a novel way to design structure-aware graph neural networks. Motivated by the limitations of traditional GNNs to grasp important topological properties of the graph, we formulate a message passing scheme enhanced with structural features that are extracted by counting the appearances of prominent substructures, as domain knowledge suggests. We show both theoretically and empirically that our construction leads to improved expressive power and attains state-of-the-art performance in real-world scenarios. In future work, we will further explore the expressivity of GSNs as an alternative to the k-WL tests, as well as their generalisation capabilities. Another important direction is to infer prominent substructures directly from the data and explore the ability of graph neural networks to compose substructures.

Broader Impact

Graph Neural Networks have shown very promising results in the analysis of graph-structured data arising in social sciences, medicine, chemistry, and physics. Our method attempts to take this field one step forward and advance the expressive power of the existing frameworks.

This research paper shares to a large extent its potential societal impacts with previous work in the interplay of Machine Learning and Network Science. Encouraging results from incorporating structural information and the ability to better exploit domain-specific knowledge, show the potential of improving current results in important applications. For instance, in the healthcare domain, there are numerous tasks that involve network data (including some of the ones that we experiment on in the main paper): molecular property prediction, drug repurposing and personalised medicine, to name a few. As mentioned before, usually these tasks correlate strongly with the underlying network structure, thus our work might allow to capture information that with previous methods would be ignored. Analogously, for social sciences, similar systems can be used to associate structural patterns with the spread of misinformation, or provide relevant news recommendations to users.

Although we do not see our method’s immediate adverse impact that goes beyond the general previous concerns about machine learning on network structured data, this should not be ignored (e.g. privacy issues when applied to large collections of personal data). Finally, regarding healthcare applications, it is necessary to make clear that our method, as most machine learning approaches at the moment, should be used as a complementary tool and its outcomes should always be accompanied with strong empirical observations (e.g. clinical trials and wide statistical studies).

References

- [1] Rex Ying, Ruining He, Kaifeng Chen, Pong Eksombatchai, William L. Hamilton, and Jure Leskovec. Graph convolutional neural networks for web-scale recommender systems. In *ACM SIGKDD International Conference on Knowledge Discovery & Data Mining (KDD)*, pages 974–983. ACM, 2018.
- [2] Alex Fout, Jonathon Byrd, Basir Shariat, and Asa Ben-Hur. Protein interface prediction using graph convolutional networks. In *Advances in Neural Information Processing Systems (NIPS)*, pages 6530–6539, 2017.
- [3] Pablo Gainza, Freyr Sverrisson, Federico Monti, Emanuele Rodola, D Boscaini, MM Bronstein, and BE Correia. Deciphering interaction fingerprints from protein molecular surfaces using geometric deep learning. *Nature Methods*, 17(2):184–192, 2020.
- [4] David Duvenaud, Dougal Maclaurin, Jorge Aguilera-Iparraguirre, Rafael Gómez-Bombarelli, Timothy Hirzel, Alán Aspuru-Guzik, and Ryan P. Adams. Convolutional networks on graphs for learning molecular fingerprints. In *Advances in Neural Information Processing Systems (NIPS)*, pages 2224–2232, 2015.
- [5] Justin Gilmer, Samuel S Schoenholz, Patrick F Riley, Oriol Vinyals, and George E Dahl. Neural message passing for quantum chemistry. In *International Conference on Machine Learning (ICML)*, volume 70 of *Proceedings of Machine Learning Research*, pages 1263–1272. PMLR, 2017.
- [6] Benjamin Sanchez-Lengeling, Jennifer N Wei, Brian K Lee, Richard C Gerkin, Alán Aspuru-Guzik, and Alexander B Wiltschko. Machine learning for scent: Learning generalizable perceptual representations of small molecules. *arXiv preprint arXiv:1910.10685*, 2019.
- [7] Thomas N. Kipf, Ethan Fetaya, Kuan-Chieh Wang, Max Welling, and Richard S. Zemel. Neural relational inference for interacting systems. In *International Conference on Machine Learning (ICML)*, volume 80 of *Proceedings of Machine Learning Research*, pages 2693–2702. PMLR, 2018.
- [8] Peter Battaglia, Razvan Pascanu, Matthew Lai, Danilo Jimenez Rezende, et al. Interaction networks for learning about objects, relations and physics. In *Advances in Neural Information Processing systems (NIPS)*, pages 4502–4510, 2016.
- [9] Jonathan Masci, Davide Boscaini, Michael M. Bronstein, and Pierre Vandergheynst. Geodesic convolutional neural networks on riemannian manifolds. In *IEEE International Conference on Computer Vision Workshops, (ICCVW)*, pages 832–840. IEEE Computer Society, 2015.
- [10] Federico Monti, Davide Boscaini, Jonathan Masci, Emanuele Rodolà, Jan Svoboda, and Michael M. Bronstein. Geometric deep learning on graphs and manifolds using mixture model cnns. In *IEEE Conference on Computer Vision and Pattern Recognition (CVPR)*, pages 5425–5434, 2017.
- [11] Giorgos Bouritsas, Sergiy Bokhnyak, Stylianos Ploumpis, Michael Bronstein, and Stefanos Zafeiriou. Neural 3d morphable models: Spiral convolutional networks for 3d shape representation learning and generation. In *Proceedings of the IEEE International Conference on Computer Vision (ICCV)*, pages 7213–7222, 2019.
- [12] Johannes Klicpera, Janek Groß, and Stephan Günnemann. Directional message passing for molecular graphs. In *International Conference on Learning Representations (ICLR)*. OpenReview.net, 2020.
- [13] Pim de Haan, Maurice Weiler, Taco Cohen, and Max Welling. Gauge equivariant mesh cnns: Anisotropic convolutions on geometric graphs. *arXiv preprint arXiv:2003.05425*, 2020.
- [14] John Ingraham, Vikas Garg, Regina Barzilay, and Tommi Jaakkola. Generative models for graph-based protein design. In *Advances in Neural Information Processing Systems (NeurIPS)*, pages 15794–15805, 2019.
- [15] Michael Schlichtkrull, Thomas N Kipf, Peter Bloem, Rianne Van Den Berg, Ivan Titov, and Max Welling. Modeling relational data with graph convolutional networks. In *European Semantic Web Conference (ESWC)*, volume 10843 of *Lecture Notes in Computer Science*, pages 593–607. Springer, 2018.
- [16] Keyulu Xu, Weihua Hu, Jure Leskovec, and Stefanie Jegelka. How powerful are graph neural networks? In *International Conference on Learning Representations (ICLR)*. OpenReview.net, 2019.
- [17] Christopher Morris, Martin Ritzert, Matthias Fey, William L Hamilton, Jan Eric Lenssen, Gaurav Rattan, and Martin Grohe. Weisfeiler and leman go neural: Higher-order graph neural networks. In *AAAI Conference on Artificial Intelligence*, pages 4602–4609. AAAI Press, 2019.
- [18] Vikraman Arvind, Frank Fuhlbrück, Johannes Köbler, and Oleg Verbitsky. On weisfeiler-leman invariance: Subgraph counts and related graph properties. In *Fundamentals of Computation Theory (FCT)*, volume 11651 of *Lecture Notes in Computer Science*, pages 111–125. Springer, 2019.
- [19] Zhengdao Chen, Lei Chen, Soledad Villar, and Joan Bruna. Can graph neural networks count substructures? *arXiv preprint arXiv:2002.04025*, 2020.
- [20] Haggai Maron, Heli Ben-Hamu, Nadav Shamir, and Yaron Lipman. Invariant and equivariant graph networks. In *International Conference on Learning Representations, (ICLR)*. OpenReview.net, 2019.

- [21] Haggai Maron, Ethan Fetaya, Nimrod Segol, and Yaron Lipman. On the universality of invariant networks. In *International Conference on Machine Learning (ICML)*, volume 97 of *Proceedings of Machine Learning Research*, pages 4363–4371. PMLR, 2019.
- [22] Haggai Maron, Heli Ben-Hamu, Hadar Serviansky, and Yaron Lipman. Provably powerful graph networks. In *Advances in Neural Information Processing Systems (NeurIPS)*, pages 2153–2164, 2019.
- [23] Vijay Prakash Dwivedi, Chaitanya K Joshi, Thomas Laurent, Yoshua Bengio, and Xavier Bresson. Benchmarking graph neural networks. *arXiv preprint arXiv:2003.00982*, 2020.
- [24] Weihua Hu, Matthias Fey, Marinka Zitnik, Yuxiao Dong, Hongyu Ren, Bowen Liu, Michele Catasta, and Jure Leskovec. Open graph benchmark: Datasets for machine learning on graphs. *arXiv preprint arXiv:2005.00687*, 2020.
- [25] Hassler Whitney. Congruent graphs and the connectivity of graphs. *American Journal of Mathematics*, 54(1):150–168, 1932.
- [26] Boris Weisfeiler and Andrei Leman. The reduction of a graph to canonical form and the algebra which appears therein. *NTI, Series 2*, 9:12–16, 1968. English translation is available at https://www.iti.zcu.cz/wl2018/pdf/wl_paper_translation.pdf.
- [27] Jin-yi Cai, Martin Fürer, and Neil Immerman. An optimal lower bound on the number of variables for graph identifications. *Combinatorica*, 12(4):389–410, 1992.
- [28] Martin Fürer. On the combinatorial power of the weisfeiler-lehman algorithm. In *International Conference on Algorithms and Complexity (CIAC)*, volume 10236 of *Lecture Notes in Computer Science*, pages 260–271. Springer, 2017.
- [29] Yann LeCun, Bernhard Boser, John S Denker, Donnie Henderson, Richard E Howard, Wayne Hubbard, and Lawrence D Jackel. Backpropagation applied to handwritten zip code recognition. *Neural computation*, 1(4):541–551, 1989.
- [30] Sainbayar Sukhbaatar, Arthur Szlam, Jason Weston, and Rob Fergus. End-to-end memory networks. In *Advances in Neural Information Processing Systems (NIPS)*, pages 2440–2448, 2015.
- [31] Jonas Gehring, Michael Auli, David Grangier, Denis Yarats, and Yann N. Dauphin. Convolutional sequence to sequence learning. In *International Conference on Machine Learning (ICML)*, volume 70 of *Proceedings of Machine Learning Research*, pages 1243–1252. PMLR, 2017.
- [32] Ashish Vaswani, Noam Shazeer, Niki Parmar, Jakob Uszkoreit, Llion Jones, Aidan N Gomez, Łukasz Kaiser, and Illia Polosukhin. Attention is all you need. In *Advances in Neural Information Processing Systems (NIPS)*, pages 5998–6008, 2017.
- [33] Ryoma Sato. A survey on the expressive power of graph neural networks. *arXiv preprint arXiv:2003.04078*, 2020.
- [34] Paul J Kelly et al. A congruence theorem for trees. *Pacific Journal of Mathematics*, 7(1):961–968, 1957.
- [35] Stanislaw M Ulam. *A collection of mathematical problems*, volume 8. Interscience Publishers, 1960.
- [36] Brendan D McKay. Small graphs are reconstructible. *Australasian J. Combinatorics*, 15:123–126, 1997.
- [37] Leslie G. Valiant. The complexity of enumeration and reliability problems. *SIAM Journal on Computing*, 8(3):410–421, 1979.
- [38] Pierre-Louis Giscard, Nils M. Kriege, and Richard C. Wilson. A general purpose algorithm for counting simple cycles and simple paths of any length. *Algorithmica*, 81(7):2716–2737, 2019.
- [39] Ryan L. Murphy, Balasubramaniam Srinivasan, Vinayak A. Rao, and Bruno Ribeiro. Relational pooling for graph representations. In *International Conference on Machine Learning (ICML)*, volume 97 of *Proceedings of Machine Learning Research*, pages 4663–4673. PMLR, 2019.
- [40] Zhengdao Chen, Soledad Villar, Lei Chen, and Joan Bruna. On the equivalence between graph isomorphism testing and function approximation with gnns. In *Advances in Neural Information Processing Systems (NeurIPS)*, pages 15868–15876, 2019.
- [41] Nicolas Keriven and Gabriel Peyré. Universal invariant and equivariant graph neural networks. In *Advances in Neural Information Processing Systems (NeurIPS)*, pages 7090–7099, 2019.
- [42] Ryoma Sato, Makoto Yamada, and Hisashi Kashima. Approximation ratios of graph neural networks for combinatorial problems. In *Advances in Neural Information Processing Systems (NeurIPS)*, pages 4083–4092, 2019.
- [43] Andreas Loukas. What graph neural networks cannot learn: depth vs width. In *International Conference on Learning Representations (ICLR)*. OpenReview.net, 2020.
- [44] Dana Angluin. Local and global properties in networks of processors. In *ACM Symposium on Theory of Computing (STOC)*, pages 82–93. ACM, 1980.

- [45] Nathan Linial. Locality in distributed graph algorithms. *SIAM Journal on Computing*, 21(1):193–201, 1992.
- [46] Moni Naor and Larry J. Stockmeyer. What can be computed locally? In *ACM Symposium on Theory of Computing (STOC)*, pages 184–193. ACM, 1993.
- [47] Ryoma Sato, Makoto Yamada, and Hisashi Kashima. Random features strengthen graph neural networks. *arXiv preprint arXiv:2002.03155*, 2020.
- [48] László Babai, Paul Erdos, and Stanley M Selkow. Random graph isomorphism. *SIAM Journal on computing*, 9(3):628–635, 1980.
- [49] Martin Fürer. On the power of combinatorial and spectral invariants. *Linear algebra and its applications*, 432(9):2373–2380, 2010.
- [50] Holger Dell, Martin Grohe, and Gaurav Rattan. Lovász meets weisfeiler and leman. In *International Colloquium on Automata, Languages, and Programming (ICALP)*, volume 107 of *LIPICs*, pages 40:1–40:14. Schloss Dagstuhl - Leibniz-Zentrum für Informatik, 2018.
- [51] Paul W Holland and Samuel Leinhardt. Local structure in social networks. *Sociological methodology*, 7:1–45, 1976.
- [52] Ron Milo, Shai Shen-Orr, Shalev Itzkovitz, Nadav Kashtan, Dmitri Chklovskii, and Uri Alon. Network motifs: simple building blocks of complex networks. *Science*, 298(5594):824–827, 2002.
- [53] Austin R Benson, David F Gleich, and Jure Leskovec. Higher-order organization of complex networks. *Science*, 353(6295):163–166, 2016.
- [54] Ashwin Paranjape, Austin R Benson, and Jure Leskovec. Motifs in temporal networks. In *ACM International Conference on Web Search and Data Mining (WSDM)*, pages 601–610. ACM, 2017.
- [55] Michihiro Kuramochi and George Karypis. Frequent subgraph discovery. In *IEEE International Conference on Data Mining (ICDM)*, pages 313–320. IEEE Computer Society, 2001.
- [56] Stefan Kramer, Luc De Raedt, and Christoph Helma. Molecular feature mining in hiv data. In *ACM SIGKDD International Conference on Knowledge Discovery & Data Mining (KDD)*, pages 136–143. ACM, 2001.
- [57] Mukund Deshpande, Michihiro Kuramochi, Nikil Wale, and George Karypis. Frequent substructure-based approaches for classifying chemical compounds. *IEEE Transactions on Knowledge and Data Engineering*, 17(8):1036–1050, 2005.
- [58] Nataša Pržulj, Derek G Corneil, and Igor Jurisica. Modeling interactome: scale-free or geometric? *Bioinformatics*, 20(18):3508–3515, 2004.
- [59] Nataša Pržulj. Biological network comparison using graphlet degree distribution. *Bioinformatics*, 23(2):177–183, 2007.
- [60] Tijana Milenković and Nataša Pržulj. Uncovering biological network function via graphlet degree signatures. *Cancer informatics*, 6:257–273, 2008.
- [61] Anida Sarajlić, Noël Malod-Dognin, Ömer Nebil Yaveroğlu, and Nataša Pržulj. Graphlet-based characterization of directed networks. *Scientific reports*, 6:35098, 2016.
- [62] Tamás Horváth, Thomas Gärtner, and Stefan Wrobel. Cyclic pattern kernels for predictive graph mining. In *ACM SIGKDD International Conference on Knowledge Discovery & Data Mining (KDD)*, pages 158–167. ACM, 2004.
- [63] Nino Shervashidze, SVN Vishwanathan, Tobias Petri, Kurt Mehlhorn, and Karsten Borgwardt. Efficient graphlet kernels for large graph comparison. In *Artificial Intelligence and Statistics (AISTATS)*, volume 5 of *Proceedings of Machine Learning Research*, pages 488–495. PMLR, 2009.
- [64] Fabrizio Costa and Kurt De Grave. Fast neighborhood subgraph pairwise distance kernel. In *International Conference on Machine Learning (ICML)*, pages 255–262. Omnipress, 2010.
- [65] Nils M. Kriege and Petra Mutzel. Subgraph matching kernels for attributed graphs. In *International Conference on Machine Learning (ICML)*, page 291–298. Omnipress, 2012.
- [66] M. R. Daredy, M. Das, and H. Yang. motif2vec: Motif aware node representation learning for heterogeneous networks. In *2019 IEEE International Conference on Big Data (Big Data)*, pages 1052–1059, 2019.
- [67] Ryan A Rossi, Nesreen K Ahmed, Eunye Koh, Sungchul Kim, Anup Rao, and Yasin Abbasi Yadkori. Hone: Higher-order network embeddings. *arXiv preprint arXiv:1801.09303*, 2018.
- [68] F. Monti, K. Otness, and M. M. Bronstein. Motifnet: A motif-based graph convolutional network for directed graphs. In *2018 IEEE Data Science Workshop (DSW)*, pages 225–228, 2018.

- [69] Aravind Sankar, Xinyang Zhang, and Kevin Chen-Chuan Chang. Meta-gnn: metagraph neural network for semi-supervised learning in attributed heterogeneous information networks. In *Proceedings of the 2019 IEEE/ACM International Conference on Advances in Social Networks Analysis and Mining (ASONAM)*, pages 137–144. ACM, 2019.
- [70] John Boaz Lee, Ryan Rossi, Xiangnan Kong, Sungchul Kim, Eunye Koh, and Anup Rao. Graph convolutional networks with motif-based attention. In *28th ACM International Conference on Information and Knowledge Management (CIKM)*, pages 499–508. ACM, 2019.
- [71] Michael Lingzhi Li, Meng Dong, Jiawei Zhou, and Alexander M Rush. A hierarchy of graph neural networks based on learnable local features. *arXiv preprint arXiv:1911.05256*, 2019.
- [72] Cheolhyeong Kim, Haeseong Moon, and Hyung Ju Hwang. Near: Neighborhood edge aggregator for graph classification. *arXiv preprint arXiv:1909.02746*, 2019.
- [73] Daniel Flam-Shepherd, Tony Wu, Pascal Friederich, and Alan Aspuru-Guzik. Neural message passing on high order paths. *Advances in Neural Information Processing Systems Workshops (NeurIPSW)*, 2020.
- [74] Muhan Zhang, Zhicheng Cui, Marion Neumann, and Yixin Chen. An end-to-end deep learning architecture for graph classification. In *AAAI Conference on Artificial Intelligence*, pages 4438–4445. AAAI Press, 2018.
- [75] Thomas Gärtner, Peter A. Flach, and Stefan Wrobel. On graph kernels: Hardness results and efficient alternatives. In *Computational Learning Theory and Kernel Machines (COLT)*, volume 2777, pages 129–143. Springer, 2003.
- [76] Marion Neumann, Roman Garnett, Christian Bauckhage, and Kristian Kersting. Propagation kernels: efficient graph kernels from propagated information. *Machine Learning*, 102(2):209–245, 2016.
- [77] Nino Shervashidze, Pascal Schweitzer, Erik Jan Van Leeuwen, Kurt Mehlhorn, and Karsten M Borgwardt. Weisfeiler-lehman graph kernels. *Journal of Machine Learning Research (JMLR)*, 12:2539–2561, 2011.
- [78] Simon S. Du, Kangcheng Hou, Ruslan Salakhutdinov, Barnabás Póczos, Ruosong Wang, and Keyulu Xu. Graph neural tangent kernel: Fusing graph neural networks with graph kernels. In *Advances in Neural Information Processing Systems (NeurIPS)*, pages 5724–5734, 2019.
- [79] James Atwood and Don Towsley. Diffusion-convolutional neural networks. In *Advances in Neural Information Processing Systems (NIPS)*, pages 1993–2001, 2016.
- [80] Sergei Ivanov, Sergei Sviridov, and Evgeny Burnaev. Understanding isomorphism bias in graph data sets. *arXiv preprint arXiv:1910.12091*, 2019.
- [81] Federico Errica, Marco Podda, Davide Bacciu, and Alessio Micheli. A fair comparison of graph neural networks for graph classification. In *International Conference on Learning Representations, ICLR*. OpenReview.net, 2020.
- [82] John J. Irwin, Teague Sterling, Michael M. Mysinger, Erin S. Bolstad, and Ryan G. Coleman. ZINC: A free tool to discover chemistry for biology. *Journal of chemical information and modeling*, 52(7):1757–1768, 2012.
- [83] Matt J. Kusner, Brooks Paige, and José Miguel Hernández-Lobato. Grammar variational autoencoder. In *International Conference on Machine Learning (ICML)*, volume 70 of *Proceedings of Machine Learning Research*, pages 1945–1954. PMLR, 2017.
- [84] Rafael Gómez-Bombarelli, Jennifer N Wei, David Duvenaud, José Miguel Hernández-Lobato, Benjamín Sánchez-Lengeling, Dennis Sheberla, Jorge Aguilera-Iparraguirre, Timothy D Hirzel, Ryan P Adams, and Alán Aspuru-Guzik. Automatic chemical design using a data-driven continuous representation of molecules. *ACS central science*, 4(2):268–276, 2018.
- [85] Wengong Jin, Regina Barzilay, and Tommi S. Jaakkola. Junction tree variational autoencoder for molecular graph generation. In *International Conference on Machine Learning (ICML)*, volume 80 of *Proceedings of Machine Learning Research*, pages 2328–2337. PMLR, 2018.
- [86] Thomas N. Kipf and Max Welling. Semi-supervised classification with graph convolutional networks. In *International Conference on Learning Representations, (ICLR)*. OpenReview.net, 2017.
- [87] Petar Velickovic, Guillem Cucurull, Arantxa Casanova, Adriana Romero, Pietro Liò, and Yoshua Bengio. Graph attention networks. In *International Conference on Learning Representations, (ICLR)*. OpenReview.net, 2018.
- [88] Xavier Bresson and Thomas Laurent. Residual gated graph convnets. *arXiv preprint arXiv:1711.07553*, 2017.
- [89] Lukas Biewald. Experiment tracking with weights and biases, 2020. Software available from wandb.com.
- [90] Adam Paszke, Sam Gross, Francisco Massa, Adam Lerer, James Bradbury, Gregory Chanan, Trevor Killeen, Zeming Lin, Natalia Gimelshein, Luca Antiga, et al. Pytorch: An imperative style, high-performance deep learning library. In *Advances in Neural Information Processing Systems (NeurIPS)*, pages 8024–8035, 2019.

- [91] Matthias Fey and Jan Eric Lenssen. Fast graph representation learning with pytorch geometric. *arXiv preprint arXiv:1903.02428*, 2019.
- [92] Keyulu Xu, Chengtao Li, Yonglong Tian, Tomohiro Sonobe, Ken-ichi Kawarabayashi, and Stefanie Jegelka. Representation learning on graphs with jumping knowledge networks. In *International Conference on Machine Learning (ICML)*, volume 80 of *Proceedings of Machine Learning Research*, pages 5449–5458. PMLR, 2018.
- [93] Pinar Yanardag and S. V. N. Vishwanathan. Deep graph kernels. In *ACM SIGKDD International Conference on Knowledge Discovery & Data Mining (KDD)*, pages 1365–1374. ACM, 2015.
- [94] Saurabh Verma and Zhi-Li Zhang. Hunt for the unique, stable, sparse and fast feature learning on graphs. In *Advances in Neural Information Processing Systems (NIPS)*, pages 88–98, 2017.
- [95] Sergey Ivanov and Evgeny Burnaev. Anonymous walk embeddings. In *International Conference on Machine Learning (ICML)*, volume 80 of *Proceedings of Machine Learning Research*, pages 2191–2200. PMLR, 2018.
- [96] Martin Simonovsky and Nikos Komodakis. Dynamic edge-conditioned filters in convolutional neural networks on graphs. In *2017 IEEE Conference on Computer Vision and Pattern Recognition (CVPR)*, pages 29–38. IEEE Computer Society, 2017.
- [97] Mathias Niepert, Mohamed Ahmed, and Konstantin Kutzkov. Learning convolutional neural networks for graphs. In *International Conference on Machine Learning (ICML)*, volume 48 of *Proceedings of Machine Learning Research*, pages 2014–2023. PMLR, 2016.
- [98] Zhitao Ying, Jiaxuan You, Christopher Morris, Xiang Ren, William L. Hamilton, and Jure Leskovec. Hierarchical graph representation learning with differentiable pooling. In *Advances in Neural Information Processing Systems (NeurIPS)*, pages 4805–4815, 2018.
- [99] Risi Kondor, Hy Truong Son, Horace Pan, Brandon M. Anderson, and Shubhendu Trivedi. Covariant compositional networks for learning graphs. In *International Conference on Learning Representations Workshops (ICLRW)*. OpenReview.net, 2018.
- [100] Zhichang Liu, Siva Krishna Mohan Nalluri, and J Fraser Stoddart. Surveying macrocyclic chemistry: from flexible crown ethers to rigid cyclophanes. *Chemical Society Reviews*, 46(9):2459–2478, 2017.
- [101] Arthur Jacot, Clément Hongler, and Franck Gabriel. Neural tangent kernel: Convergence and generalization in neural networks. In *Advances in Neural Information Processing Systems (NeurIPS)*, pages 8580–8589, 2018.
- [102] Zeyuan Allen-Zhu, Yuanzhi Li, and Zhao Song. A convergence theory for deep learning via over-parameterization. In *International Conference on Machine Learning (ICML)*, volume 97 of *Proceedings of Machine Learning Research*, pages 242–252. PMLR, 2019.
- [103] Simon S. Du, Jason D. Lee, Haochuan Li, Liwei Wang, and Xiyu Zhai. Gradient descent finds global minima of deep neural networks. In *International Conference on Machine Learning (ICML)*, volume 97 of *Proceedings of Machine Learning Research*, pages 1675–1685. PMLR, 2019.
- [104] Minjie Wang, Lingfan Yu, Da Zheng, Quan Gan, Yu Gai, Zihao Ye, Mufei Li, Jinjing Zhou, Qi Huang, Chao Ma, Ziyue Huang, Qipeng Guo, Hao Zhang, Haibin Lin, Junbo Zhao, Jinyang Li, Alexander J. Smola, and Zheng Zhang. Deep graph library: Towards efficient and scalable deep learning on graphs. *arXiv preprint arXiv:1909.01315*, 2019.

A Proofs - Additional Details

A.1 Proposition 3.1 (2nd part): GSNs are at least as powerful as the 1-WL test

Proof. We will show the above statement for node-labelled graphs, since traditionally the 1-WL test does not take into account edge labels.⁶ We can rephrase the statement as follows: *If GSN deems two graphs G_1, G_2 as isomorphic, then also 1-WL deems them isomorphic.* Given that the graph-level representation is extracted by a readout function that receives the multiset of the node colours in its input (i.e. the graph-level representation is the node colour histogram at some iteration t), then it suffices to show that if for the two graphs the multiset of the node colours that GSN infers is the same, then also 1-WL will infer the same multiset for the two graphs.

Consider the case where the two multisets that GSN extracts are the same: i.e. $\mathcal{I}(\mathbf{h}^t(v))_{v \in \mathcal{V}_{G_1}} = \mathcal{I}(\mathbf{h}^t(u))_{u \in \mathcal{V}_{G_2}}$. Then both multisets contain the same distinct colour/hidden representations with the exact same multiplicity. Thus, it further suffices to show that if two nodes v, u (that may belong to the same or to different graphs) have the same GSN hidden representations $\mathbf{h}^t(v) = \mathbf{h}^t(u)$ at any iteration t , then they will also have the same colours $c^t(v) = c^t(u)$, extracted by 1-WL. Intuitively, this means that GSN creates a partition of the nodes of each graph that is at least as fine-grained as the one created by 1-WL. We prove by induction (similarly to [16]) that GSN model class contains a model where this holds (w.l.o.g. we show that for GSN-v; same proof applies to GSN-e).

For $t = 0$ the statement holds since the initial node features are the same for both GSN and 1-WL, i.e. $\mathbf{h}^0(v) = c^0(v)$, $\forall v \in \mathcal{V}_{G_1} \cup \mathcal{V}_{G_2}$. Suppose the statement holds for $t - 1$, i.e. $\mathbf{h}^{t-1}(v) = \mathbf{h}^{t-1}(u) \Rightarrow c^{t-1}(v) = c^{t-1}(u)$. Then we show that it also holds for t .

Every node hidden representation at step t is updated as follows: $\mathbf{h}^t(v) = \text{UP}^t(\mathbf{h}^{t-1}(v), \text{MSG}^t(v))$. Assuming that the update function UP^t is injective, we have the following: if $\mathbf{h}^t(v) = \mathbf{h}^t(u)$, then:

1. $\mathbf{h}^{t-1}(v) = \mathbf{h}^{t-1}(u)$, which from the induction hypothesis implies that $c^{t-1}(v) = c^{t-1}(u)$.
2. $\text{MSG}^t(v) = \text{MSG}^t(u)$, where the message function is defined as in Eq. 5 of the main paper: $\text{MSG}^t(v) = \sum_{w \in \mathcal{N}(v)} M^t(\mathbf{h}^{t-1}(v), \mathbf{h}^{t-1}(w), \mathbf{x}_V(v), \mathbf{x}_V(w))$. Additionally here we require MSG^t to be injective w.r.t. the multiset of the hidden representations of the neighbours. In fact, using Lemma 5 from [16] we know that there always exists a function M^t , such that $\text{MSG}^t(v)$ is unique for each multiset $\mathcal{I}(\mathbf{h}^{t-1}(v), \mathbf{h}^{t-1}(w), \mathbf{x}_V(v), \mathbf{x}_V(w))_{w \in \mathcal{N}_v}$, assuming that the domain from where the elements of the multiset originate is countable. Thus,

$$\begin{aligned} \text{MSG}^t(v) = \text{MSG}^t(u) &\Rightarrow \\ \mathcal{I}(\mathbf{h}^{t-1}(v), \mathbf{h}^{t-1}(w), \mathbf{x}_V(v), \mathbf{x}_V(w))_{w \in \mathcal{N}_v} &= \mathcal{I}(\mathbf{h}^{t-1}(u), \mathbf{h}^{t-1}(z), \mathbf{x}_V(u), \mathbf{x}_V(z))_{z \in \mathcal{N}_u} \Rightarrow \\ \mathcal{I}(\mathbf{h}^{t-1}(v), \mathbf{h}^{t-1}(w))_{w \in \mathcal{N}_v} &= \mathcal{I}(\mathbf{h}^{t-1}(u), \mathbf{h}^{t-1}(z))_{z \in \mathcal{N}_u} \end{aligned}$$

From the induction hypothesis we know that $\mathbf{h}^{t-1}(w) = \mathbf{h}^{t-1}(z)$ implies that $c^{t-1}(w) = c^{t-1}(z)$ for any $w \in \mathcal{N}_v, z \in \mathcal{N}_u$, thus $\mathcal{I}(c^{t-1}(w))_{w \in \mathcal{N}_v} = \mathcal{I}(c^{t-1}(z))_{z \in \mathcal{N}_u}$.

Concluding, given the update rule of 1-WL: $c^t(v) = \text{HASH}(c^{t-1}(v), \mathcal{I}(c^{t-1}(w))_{w \in \mathcal{N}_v})$, it holds that $c^t(v) = c^t(u)$.

□

A.2 Why does 2-FWL fail on strongly regular graphs?

Below we provide a proof for this known statement in order to give further intuition in the limitations of the 2-FWL. We first rigorously describe what an isomorphism type is. Two k-tuples $\mathbf{v}^a = \{v_1^a, v_2^a, \dots, v_k^a\}$, $\mathbf{v}^b = \{v_1^b, v_2^b, \dots, v_k^b\}$ will have the same isomorphism type iff:

⁶if one considers a simple 1-WL extension that concatenates edge labels to neighbour colours, then the same proof applies.

- $\forall i, j \in \{0, 1, \dots, k\}, \quad v_i^a = v_j^a \Leftrightarrow v_i^b = v_j^b$
- $\forall i, j \in \{0, 1, \dots, k\}, \quad v_i^a \sim v_j^a \Leftrightarrow v_i^b \sim v_j^b$, where \sim means that the vertices are adjacent.

Note that this is a stronger condition than isomorphism, since the mapping between the vertices of the two tuples needs to preserve order. In case the graph is employed with edge and vertex features, they need to be preserved as well (see [19]) for the extended case).

For the 2-FWL test, when working with simple undirected graphs without self-loops, we have the following 2-tuple isomorphism types:

- $\mathbf{v} = \{v_1, v_1\}$: *vertex type*. Mapped to the colour $c^{(0)} = c_\alpha$
- $\mathbf{v} = \{v_1, v_2\}$ and $v_1 \not\sim v_2$: *non-edge type*. Mapped to the colour $c^{(0)} = c_\beta$
- $\mathbf{v} = \{v_1, v_2\}$ and $v_1 \sim v_2$: *edge type*. Mapped to the colour $c^{(0)} = c_\gamma$

For each 2-tuple $\mathbf{v} = \{v_1, v_2\}$, a generalised “neighbour” is the following tuple: $(\mathbf{v}_{u,1}, \mathbf{v}_{u,2}) = ((u, v_2), (v_1, u))$, where u is an arbitrary vertex in the graph.

Now, let us consider a strongly regular graph $\text{SR}(n, d, \lambda, \mu)$. We have the following cases:

- generalised neighbour of a *vertex type* tuple: $(\mathbf{v}_{u,1}, \mathbf{v}_{u,2}) = ((u, v_1), (v_1, u))$. The corresponding neighbour colour tuples are:
 - (c_α, c_α) if $v_1 = u$,
 - (c_β, c_β) if $v_1 \not\sim u$,
 - (c_γ, c_γ) if $v_1 \sim u$.

The update of the 2-FWL is: $c^{(1)}(\mathbf{v}) = \text{HASH}\left(c_\alpha, \underbrace{(c_\alpha, c_\alpha)}_{1 \text{ time}}, \underbrace{(c_\beta, c_\beta)}_{n-1-d \text{ times}}, \underbrace{(c_\gamma, c_\gamma)}_{d \text{ times}}\right)$

same for all *vertex type* 2-tuples.

- generalised neighbour of a *non-edge type* tuple: $(\mathbf{v}_{u,1}, \mathbf{v}_{u,2}) = ((u, v_2), (v_1, u))$. The corresponding neighbour colour tuples are:
 - (c_α, c_β) if $v_2 = u$,
 - (c_β, c_α) if $v_1 = u$,
 - (c_γ, c_β) if $v_2 \sim u$ and $v_1 \not\sim u$,
 - (c_β, c_γ) if $v_1 \sim u$ and $v_2 \not\sim u$,
 - (c_β, c_β) if $v_1 \not\sim u$ and $v_2 \not\sim u$,
 - (c_γ, c_γ) if $v_1 \sim u$ and $v_2 \sim u$.

The update of the 2-FWL is:

$c^{(1)}(\mathbf{v}) = \text{HASH}\left(c_\beta, \underbrace{(c_\alpha, c_\beta)}_{1 \text{ time}}, \underbrace{(c_\beta, c_\alpha)}_{1 \text{ time}}, \underbrace{(c_\gamma, c_\beta)}_{d-\mu \text{ times}}, \underbrace{(c_\beta, c_\gamma)}_{d-\mu \text{ times}}, \underbrace{(c_\beta, c_\beta)}_{n-2-(2d-\mu) \text{ times}}, \underbrace{(c_\gamma, c_\gamma)}_{\mu \text{ times}}\right)$

same for all *non-edge type* 2-tuples.

- generalised neighbour of an *edge type* tuple:
 - (c_α, c_γ) if $v_2 = u$,
 - (c_γ, c_α) if $v_1 = u$,
 - (c_γ, c_β) if $v_2 \sim u$ and $v_1 \not\sim u$,
 - (c_β, c_γ) if $v_1 \sim u$ and $v_2 \not\sim u$,
 - (c_β, c_β) if $v_1 \not\sim u$ and $v_2 \not\sim u$,
 - (c_γ, c_γ) if $v_1 \sim u$ and $v_2 \sim u$.

The update of the 2-FWL is:

$c^{(1)}(\mathbf{v}) = \text{HASH}\left(c_\gamma, \underbrace{(c_\alpha, c_\gamma)}_{1 \text{ time}}, \underbrace{(c_\gamma, c_\alpha)}_{1 \text{ time}}, \underbrace{(c_\gamma, c_\beta)}_{d-\lambda \text{ times}}, \underbrace{(c_\beta, c_\gamma)}_{d-\lambda \text{ times}}, \underbrace{(c_\beta, c_\beta)}_{n-2-(2d-\lambda) \text{ times}}, \underbrace{(c_\gamma, c_\gamma)}_{\lambda \text{ times}}\right)$

same for all *edge type* 2-tuples.

From the analysis above, it is clear that all 2-tuples in the graph of the same initial type are assigned the same colour in the 1st iteration of 2-FWL. In other words, the vertices cannot be furthered partitioned, so the algorithm terminates. Therefore, if two SR graphs have the same parameters n, d, λ, μ then 2-FWL will yield the same colour distribution and thus the graphs will be deemed isomorphic.

B Experiments

In the following appendix we give the implementation details of the experimental section. All experiments were performed on a server equipped with 8 Tesla V100 16 GB GPUs, except for the Collab dataset where a Tesla V100 GPU with 32 GB RAM was used due to larger memory requirements (a large percentage of Collab graphs are dense or even nearly complete in some cases). Experimental tracking and hyperparameter optimisation were done via the Weights & Biases platform (wandb) [89]. Our implementation is based on native PyTorch sparse operations [90] in order to ensure complete reproducibility of the results. PyTorch Geometric [91] was used for additional operations (such as preprocessing and data loading).

In each one of the different experiments we aim to show that structural identifiers can be used off-the-shelf and are independent of the architecture. At the same time we aim to suppress the effect of other confounding factors in the model performance, thus wherever possible we build our model on top of a baseline architecture. More details in the relevant subsections. Interestingly, we observed that in most of the cases it was sufficient to replace only the first layer of the baseline architecture with a GSN layer, in order to obtain a boost in performance. This can be understood by considering that if the update and message functions are sufficiently expressive, then they should be able to learn to preserve the input information in their output (in the hidden states of the vertices with regards to vertex counts, or in the hidden states of the endpoints of the edges with regards to edge counts).

Throughout the experimental evaluation the structural identifiers $\mathbf{x}_V(v)$ and $\mathbf{x}_E(\{u, v\})$ are one-hot encoded, by taking into account the unique count values present in the dataset. Other more sophisticated methods can be used, e.g. transformation to continuous features via a normalisation scheme or binning. However, we found that the number of unique values in our datasets were usually relatively small (which is a good indication of recurrent structural roles) and thus such methods were not necessary.

B.1 Synthetic Experiment

For the Strongly Regular graphs dataset we use all the available families of graphs with size of at most 35 nodes:

- SR(16,6,2,2): 2 graphs
- SR(25,12,5,6): 15 graphs
- SR(26,10,3,4): 10 graphs
- SR(28,12,6,4): 4 graphs
- SR(29,14,6,7): 41 graphs
- SR(35,16,6,8): 3854 graphs
- SR(35,18,9,9): 227 graphs

The total number of non-isomorphic pairs of the same size is $\approx 7 * 10^7$. We used a simple 2-layer architecture with width 64. The message aggregation was performed as in the general formulation of Eq. 5 and 6 of the main paper, where the update and the message functions are MLPs. The prediction is inferred by applying a sum readout function in the last layer (i.e. a graph-level representation is obtained by summing the node-level representations) and then passing the output through a MLP (we did not use jumping knowledge from intermediate layers [92]). Regarding the substructures, we use *graphlet* counting, as certain *motifs* (e.g. cycles of length up to 7) are known to be unable to distinguish strongly regular graphs (since they can be counted by the 2-FWL [28, 18]).

Given the adversities that strongly regular graphs pose in graph isomorphism testing, it would be interesting to see how this method can perform in other categories of hard instances, such as the

Table 4: Graph Classification accuracy on various social and biological networks from the TUD Datasets collection <https://chrsmrrs.github.io/datasets/>. Graph Kernel methods are denoted with an *. For completeness we also include methods that were evaluated on potentially different splits. The top three performance scores are highlighted as: **First**, **Second**, **Third**.

Dataset	MUTAG	PTC	Proteins	NCI1	Collab	IMDB-B	IMDB-M	
size	188	344	1113	4110	5000	1000	1500	
classes	2	2	2	2	3	2	3	
avg num. nodes	17.9	25.5	39.1	29.8	74.4	19.7	13	
different splits	DGK* (best) [93]	87.4 ±2.7	60.1±2.6	75.7±0.5	80.3 ±0.5	73.1 ±0.3	67.0±0.6	44.6±0.5
	FSGD* [94]	92.1±	62.8±	73.4±	79.8±	80.0±	73.6±	52.4±
	AWE-FB*[95]	87.9±9.8	N/A	N/A	N/A	71.0±1.5	73.1±3.3	51.6±4.7
	AWE-DD*[95]	N/A	N/A	N/A	N/A	73.9±1.9	74.5±5.8	51.5±3.6
	ECC [96]	76.1±	N/A	N/A	76.8±	N/A	N/A	N/A
	PSCN k=10 ^E [97]	92.6±4.2	60.0±4.8	75.9±2.8	78.6±1.9	72.6±2.2	71.0±2.3	45.2±2.8
	DiffPool [98]	N/A	N/A	76.2±	N/A	75.5 ±	N/A	N/A
	CCN [99]	91.6±7.2	70.6±7.0	N/A	76.3±4.1	N/A	NA	N/A
	1-2-3 GNN [17]	86.1±	60.9±	75.5±	76.2±	N/A	74.2±	49.5±
same splits	RWK* [75]	79.2±2.1	55.9±0.3	59.6±0.1	>3 days	N/A	N/A	N/A
	GK* (k=3) [63]	81.4±1.7	55.7±0.5	71.4±0.31	62.5±0.3	N/A	N/A	N/A
	PK* [76]	76.0±2.7	59.5±2.4	73.7±0.7	82.5±0.5	N/A	N/A	N/A
	WL kernel* [77]	90.4±5.7	59.9±4.3	75.0±3.1	86.0±1.8	78.9±1.9	73.8±3.9	50.9±3.8
	GNTK* [78]	90.0±8.5	67.9±6.9	75.6±4.2	84.2±1.5	83.6±1.0	76.9±3.6	52.8±4.6
	DCNN [79]	N/A	N/A	61.3±1.6	56.6±1.0	52.1±0.7	49.1±1.4	33.5±1.4
	DGCNN [74]	85.8±1.8	58.6±2.5	75.5±0.9	74.4±0.5	73.8±0.5	70.0±0.9	47.8±0.9
	IGN [20]	83.9±13.	58.5±6.9	76.6±5.5	74.3±2.7	78.3±2.5	72.0±5.5	48.7±3.4
	GIN [16]	89.4±5.6	64.6±7.0	76.2±2.8	82.7±1.7	80.2±1.9	75.1±5.1	52.3±2.8
	PPGNs [22]	90.6±8.7	66.2±6.6	77.2±4.7	83.2±1.1	81.4±1.4	73.0±5.8	50.5±3.6
	GSN-e (Ours)	90.6±7.5	68.2±7.2	76.6±5.0	83.5±2.3	85.5±1.2	77.8±3.3	54.3±3.3
		6 (cycles)	6 (cycles)	4 (cliques)	15 (cycles)	3 (triangles)	5 (cliques)	5 (cliques)
GSN-v (Ours)	92.2±7.5	67.4±5.7	74.6±5.0	83.5±2.0	82.7±1.5	76.8±2.0	52.6±3.6	
	12 (cycles)	10 (cycles)	4 (cliques)	3 (triangles)	3 (triangles)	4 (cliques)	3 (cliques)	

classical *CFI* counter-examples for k-WL proposed in [27], and explore further its expressive power and combinatorial properties. We leave this direction to future work.

B.2 TUD Graph Classification Benchmarks

For this family of experiments, due to the usually small size of the datasets, we choose a parameter-efficient architecture, in order to reduce the risk of overfitting. In particular, we follow the simple GIN architecture [16] and we concatenate structural identifiers to node or edge features depending on the variant. Then for GSN-v, the hidden representation is updated as follows:

$$\mathbf{h}^{t+1}(v) = \text{UP}^{t+1}\left(\left[\mathbf{h}^t(v); \mathbf{x}_V(v)\right] + \sum_{u \in \mathcal{N}_v} \left[\mathbf{h}^t(u); \mathbf{x}_V(u)\right]\right), \quad (7)$$

and for GSN-e:

$$\mathbf{h}^{t+1}(v) = \text{UP}^{t+1}\left(\left[\mathbf{h}^t(v); \mathbf{x}_E(\{v, v\})\right] + \sum_{u \in \mathcal{N}_v} \left[\mathbf{h}^t(u); \mathbf{x}_E(\{u, v\})\right]\right), \quad (8)$$

where $\mathbf{x}_E(\{v, v\})$ is a dummy variable (also one-hot encoded) used to distinguish self-loops from edges. Empirically, we did not find training the ϵ parameter used in GIN to make a difference. Note that this architecture is less expressive than our general formulation. However, we found it to work well in practice for the TUD datasets, possibly due to its simplicity and small number of parameters.

We implement an architecture similar to GIN [16], i.e. 4 message passing layers, jumping knowledge from all the layers [92] (including the input), transformation of each intermediate graph-level representation by a linear layer, sum readout for biological and mean readout for social networks. Node features are one-hot encodings of the categorical node labels. Similarly to the baseline, the hyperparameters search space is the following: batch size in {32, 128} (except for Collab where only 32 was searched due to GPU memory limits), dropout in {0,0.5}, network width in {16,32} for biological networks, 64 for social networks, learning rate in {0.01, 0.001}, decay rate in {0.5,0.9} and decay steps in {10,50} (number of epochs after which the learning rate is reduced by multiplying

Table 5: Chosen hyperparameters for each of the two GSN variants for each dataset.

Dataset	MUTAG	PTC	Proteins	NCI1	Collab	IMDB-B	IMDB-M
GSN-e	batch size	32	128	32	32	32	32
	width	32	16	32	32	64	64
	decay rate	0.9	0.5	0.5	0.9	0.5	0.5
	decay steps	50	50	10	10	50	10
	dropout	0.5	0	0/5	0	0	0
	lr	10^{-3}	10^{-3}	10^{-2}	10^{-3}	10^{-2}	10^{-3}
	degree	No	No	No	No	No	Yes
	substructure type	graphlets	motifs	same	graphlets	same	same
	substructure family	cycles	cycles	cliques	cycles	clique	cliques
	k	6	6	4	15	3	5
GSN-v	batch size	32	128	32	32	32	32
	width	32	16	32	32	64	64
	decay rate	0.9	0.5	0.5	0.9	0.5	0.5
	decay steps	50	50	10	10	50	10
	dropout	0.5	0	0.5	0	0	0
	lr	10^{-3}	10^{-3}	10^{-2}	10^{-3}	10^{-2}	10^{-3}
	degree	No	No	No	No	Yes	Yes
	substructure type	graphlets	graphlets	same	same	same	same
	substructure family	cycles	cycles	cliques	cycles	cliques	cliques
	k	12	10	4	3	3	4

with the decay rate). For social networks, since they are not attributed graphs, we also experimented with using the degree as a node feature, but in most cases the structural identifiers were sufficient.

Model selection is done in two stages. First, we choose a substructure that we perceive as promising based on indications from the specific domain: *triangles* for social networks and Proteins, and *6-cycles (motifs)* for molecules. Under this setting we tune model hyperparameters for a GSN-e model. Then, we extend our search to the parameters related to the substructure collection: i.e. the maximum size k and motifs against graphlets. In all the molecular datasets we search cycles with $k = 3, \dots, 12$, except for NCI1, where we also consider larger sizes due to the presence of large rings in the dataset (*macrocycles* [100]). For social networks, we searched cliques with $k = 3, 4, 5$. In Table 5 we report the hyperparameters chosen by our model selection procedure, including the best performing substructures.

The seven datasets⁷ we chose are the intersection of the datasets used by the authors of our main baselines: the Graph Isomorphism Network (GIN) [16], a simple, yet powerful GNN with expressive power equal to the 1-WL test, and the Provably Powerful Graph Network (PPGN) [22], a polynomial alternative to the Invariant Graph Network [20], that increases its expressive power to match the 2-FWL. We also compare our results to other GNNs as well as Graph Kernel approaches. Our main baseline from the GK family is the Graph Neural Tangent Kernel (GNTK) [78], which is a kernel obtained from a GNN of infinite width. This operates in the Neural Tangent Kernel regime [101, 102, 103].

Table 4 is an extended version of Table 1 of the main paper, where the most prominent methods are reported, regardless of the splits they were evaluated on. For DGK (best variant) [93], FSGD [94], AWE [95], ECC [96], PSCN [97], DiffPool [98], CCN [99] (slightly different setting since they perform a train, validation, test split), 1-2-3 GNN [17] and GNTK [78], we obtain the results from the original papers. For RWK [75], GK [63], PK [76], DCNN [79] and DGCNN [74], we obtain the results from the DGCNN paper, where the authors reimplemented these methods and evaluated them with the same split. Similarly, we obtain the WLK [77] and GIN [16] results from the GIN paper, and IGN [20] and PPGN [22] results from the PPGN paper.

B.3 Graph Regression on ZINC

The ZINC dataset includes 12k molecular graphs of which 10k form the training set and the remaining 2k are equally split between validation and test (splits obtained from <https://github.com/graphdeeplearning/benchmarking-gnns>). Molecule sizes range from 9 to 37 nodes/atoms.

⁷more details on the description of the datasets and the corresponding tasks can be found at [16].

Table 6: Chosen substructures for ZINC

Model	GIN [†]	MPNN ^E	GSN	GSN ^E
features	-	-	edges (GSN-e)	vertices (GSN-v)
substructure type	-	-	graphlets	motifs
substructure family	-	-	cycles	cycles
k	-	-	10	8

Node features encode the type of atoms and edge features the chemical bonds between them. Again, here node and edge features are one-hot encoded.

We re-implemented the GIN baseline (GIN[†] in Table 2 of the main paper) due to the fact that the authors of [23], from whom we obtained the baseline results and evaluation procedure, used the DGL [104] framework, while we used native PyTorch sparse operations, to which we attribute a discrepancy in the results. We extended GIN with structural identifiers as in Eq. 7 and 8 (GSN model in Table 2). Our stronger baseline (MPNN^E model in Table 2) updates node representations as follows: $\mathbf{h}^{t+1}(v) = \text{UP}^{t+1}(\mathbf{h}^t(v), \text{MSG}^{t+1}(v))$,

$$\text{MSG}^{t+1}(v) = \sum_{u \in \mathcal{N}(v)} M^t(\mathbf{h}^t(v), \mathbf{h}^t(u), \mathbf{e}(\{u, v\})) \quad (9)$$

$$\text{MSG}^{t+1}(v) = \sum_{u \in \mathcal{N}(v)} M^t(\mathbf{h}^t(v), \mathbf{h}^t(u), \mathbf{e}(\{u, v\})), \quad (10)$$

where UP^t and M^t functions are MLPs and $\mathbf{e}(\{u, v\})$ are edge features. Our extension with structural identifiers (GSN^E model in Table 2) is precisely the model of Eq. 5 or 6 of the main paper. Observe that, probably due to the fact that the ZINC dataset is larger and more stable, the general MPNN-based formulation performs better than the GIN-based counterpart.

Following the same rationale as before, the network configuration is minimally modified w.r.t. the baseline of [23], while here no hyperparameter tuning is done, since the best performing hyperparameters are provided by the authors. In particular, the parameters are the following: 4 message passing layers, no jumping knowledge, transformation of the output of the last layer by a MLP, readout: sum, batch size: 128, dropout: 0.0, network width: 128, learning rate: 0.001. The learning rate is reduced by 0.5 (decay rate) after 5 epochs (patience) without improvement in the validation loss. Training is stopped when the learning rate reaches the minimum learning rate value of 10^{-5} .

We select our best performing substructure related parameters based on the performance in the validation set in the last epoch. We search cycles with $k = 3, \dots, 10$, graphlets against motifs, and GSN-v against GSN-e (see Table 6 for the chosen parameters). Once the model is chosen, we repeat the experiment 10 times with different seeds and report the mean and standard deviation of the test MAE in the last epoch. This is performed for all 4 models that we implemented and compared (GIN[†], MPNN^E, GSN, GSN^E).

B.4 Graph Classification on ogbg-molhiv

The ogbg-molhiv dataset contains $\approx 41\text{K}$ graphs, with 25.5 nodes and 27.5 edges on average. As most molecular graphs, the average degree is small (2.2) and they exhibit a tree-like structure (average clustering coefficient 0.002). The average diameter is 12 (more details in [24]).

We follow the design choices of the authors of [24] and extend their architectures to include structural identifiers. Initial node features and edge features are multi-hot encodings passed through linear layers that project them in the same embedding space, i.e. $\mathbf{h}^0(v) = \mathbf{W}_h^0 \cdot \mathbf{h}_{in}(v)$, $\mathbf{e}^t(\{v, u\}) = \mathbf{W}_e^t \cdot \mathbf{e}_{in}(\{u, v\})$. The baseline model is a modification of GIN that allows for edge features: for each neighbour, the hidden representation is added to an embedding of its associated edge feature. Then the result is passed through a ReLU non-linearity which produces the neighbour’s

Table 7: Chosen substructures for ogbg-molhiv

Model	GSN-AF	GSN-VN	GSN-VN -AF
features	edges (GSN-e)	vertices (GSN-v)	edges (GSN-e)
substructure type	graphlets	graphlets	graphlets
substructure family	cycles	cycles	cycles
k	12	6	6

message. Formally, the aggregation is as follows:

$$\mathbf{h}^{t+1}(v) = \text{UP}^{t+1} \left(\mathbf{h}^t(v) + \sum_{u \in \mathcal{N}_v} \sigma(\mathbf{h}^t(u) + \mathbf{e}^t(\{v, u\})) \right) \quad (11)$$

A stronger baseline is also proposed by the authors: in order to allow global information to be broadcasted to the nodes, a *virtual node* takes part in the message passing (-VN setting in Table 3 of the main paper). The virtual node representation, denoted as \mathbf{G}^t , is initialised as a zero vector \mathbf{G}^0 and then Message Passing proceeds as follows:

$$\begin{aligned} \tilde{\mathbf{h}}_v^t &= \mathbf{h}^t(v) + \mathbf{G}^t, \quad \mathbf{h}^{t+1}(v) = \text{UP}^{t+1} \left(\tilde{\mathbf{h}}^t(v) + \sum_{u \in \mathcal{N}_v} \sigma(\tilde{\mathbf{h}}^t(u) + \mathbf{e}^t(\{v, u\})) \right), \\ \mathbf{G}^{t+1} &= \text{MLP}^{t+1} \left(\mathbf{G}^t + \sum_{u \in \mathcal{N}_v} \tilde{\mathbf{h}}^t(u) \right) \end{aligned} \quad (12)$$

We modify this model, as follows: first the substructure counts are embedded into the same embedding space as the rest of the features. Then, for GSN-v, they are added to the corresponding node embeddings: $\hat{\mathbf{h}}^t(v) = \mathbf{h}^t(v) + \mathbf{W}_V^t \cdot \mathbf{x}_V(v)$, or for GSN-e, they are added to the edge embeddings $\hat{\mathbf{e}}^t(\{v, u\}) = \mathbf{e}^t(\{v, u\}) + \mathbf{W}_E^t \cdot \mathbf{x}_E(\{u, v\})$. Interestingly, even with this simple modification we obtain a considerable improvement in the performance of the model in all splits, thus demonstrating strong generalisation capabilities.

We use the same hyperparameters as the ones provided by the authors, i.e. 5 message passing layers, no jumping knowledge, mean readout, a linear layer applied after the readout, batch size: 32, dropout: 0.5, network width/embedding dimension: 300 (in the ogb implementation the hidden layer of each MLP has dimensions equal to 2*network width, contrary to the rest of the experiments where network width and MLP hidden dimensions are equal), learning rate: 0.001.

We select our best performing substructure related parameters based on the highest validation ROC-AUC (choosing the best scoring epoch as in [24]). We search cycles with $k = 3, \dots, 12$, graphlets against motifs, and GSN-v against GSN-e (see Table 7 for the chosen parameters). We repeat the experiment 10 times with different seeds and report the mean and standard deviation of the train, validation and test ROC-AUC, again by choosing the best scoring epoch w.r.t the validation set. We repeat the process for all 3 settings independently (GSN-VN, GSN-AF, GSN-VN-AF).